

A Class-Aware Representation Refinement Framework for Graph Classification

Jiaxing Xu, Jinjie Ni, Sophi Shilpa Gururajapathy & Yiping Ke

Nanyang Technological University, Singapore

{jiaxing.xu, jinjie001, sophi.sg, ypke}@ntu.edu.sg

Abstract—Graph Neural Networks (GNNs) are widely used for graph representation learning. Despite its prevalence, GNN suffers from two drawbacks in the graph classification task, the neglect of graph-level relationships, and the generalization issue. Each graph is treated separately in GNN message passing/graph pooling, and existing methods to address overfitting operate on each individual graph. This makes the graph representations learnt less effective in the downstream classification. In this paper, we propose a Class-Aware Representation rEfinement (CARE) framework for the task of graph classification. CARE computes simple yet powerful class representations and injects them to steer the learning of graph representations towards better class separability. CARE is a plug-and-play framework that is highly flexible and able to incorporate arbitrary GNN backbones without significantly increasing the computational cost. We also theoretically prove that CARE has a better generalization upper bound than its GNN backbone through Vapnik-Chervonenkis (VC) dimension analysis. Our extensive experiments with 10 well-known GNN backbones on 9 benchmark datasets validate the superiority and effectiveness of CARE over its GNN counterparts.

Index Terms—Graph Neural Network, Representation Learning, Graph Classification

I. INTRODUCTION

In recent years, Graph Neural Networks (GNNs) have attracted a surge of attention and been extensively used to learn graph representations for downstream tasks such as graph classification [1], [2], link prediction [3], graph clustering [4], [5], etc. They have been applied to graph structured data from a wide range of application domains, including social networks [6]–[8], molecular data [9], [10], recommendation system [11], [12], brain networks [13], and many more.

The GNN-based graph representation learning has two main steps. It first passes the input graphs to GNN to obtain node representations. It then uses a down-sampling strategy [14], also known as graph pooling [7], [10], to aggregate and transform node representations to graph representations. This approach suffers from two major drawbacks when applied to the downstream classification task: (1) Neglect of graph-level relationships; and (2) Generalization issue.

Neglect of graph-level relationships. Existing GNN architectures consider each input graph independently in their training processes. Input graphs are passed individually to GNN to yield node representations. In addition, the model also treats each graph separately in its design of loss. The relationships (similarity and/or discrepancy) among different input graphs are fully neglected. Though the model parameters are trained

by the set of input graphs collectively, it is done through a long pathway from node representations to graph representations and finally to the loss. As a result, the effectiveness of the model will be significantly compromised when applied to the downstream classification. With molecular data, for instance, one would want the molecules from the same class to share similar representations. This is natural as molecules belonging to the same class often carry certain common substructures (e.g., the same set of functional groups). These substructures could be class-specific and serve as a perfect signature of a class. Without considering such graph-level information, the graph representations learnt would be less effective in separating different graph classes.

Generalization issue. This is an inherent issue in GNN that the model tends to overfit when the network gets deeper or the hidden dimensionality gets larger [15]. Some methods have been proposed to alleviate this issue. Several graph-argumentation based methods improve the generalization ability by modifying input graphs [16], or generating new graphs for adversarial learning [17] and contrastive learning [18]. Some other works [19], [20] resample or reweight data instances to remit the overfitting problem. However, these methods operate on each individual graph and fail to explore the effectiveness of graph-level information in improving generalization.

In this paper, we develop a Class-Aware Representation rEfinement (CARE) framework to address the two above-mentioned limitations of GNNs on the task of graph classification. Built upon the two existing steps of GNN models for node representation learning and graph pooling, we introduce a new block for extracting class-specific information, namely the Class-Aware Refiner. The idea of this refiner is simple but effective. Under the supervision of ground-truth labels, the refiner learns the class representation from a bag of subgraph representations (generated by graph pooling) from each class, and uses it to refine the representation of each graph within the same class. In this way, we inject the class-specific information to graph representations, with the hope that it can steer the graph representation learning to reflect class signatures. Inspired by the separability in clustering [21], we also propose a class loss that takes into account intra-class graph similarity and inter-class graph discrepancy. This class loss is combined with the classification loss to directly influence the training of class representations to gain better class separability. We further design two different architectures

of CARE so that our framework can incorporate arbitrary GNN backbones. In terms of the model generalization, we analyze the Vapnik-Chervonenkis (VC) dimension [22] of CARE and provide theoretic guarantee that the upper bound of the VC dimension of CARE is lower than that of the GNN backbone. The better ability of CARE in alleviating overfitting is also evidenced in our experiments.

We empirically validate the graph classification performance of CARE on 9 benchmark datasets with 10 commonly used GNN backbones. The results demonstrate that CARE significantly outperforms its GNN backbones: it achieves up to 11% improvement in classification accuracy. We also perform a series of ablation studies to assess the effect of each component. We use a case study to showcase that the graph representations refined by CARE is able to achieve better class separability. Though CARE introduces an additional refiner to the backbone model, our results show that the consideration of graph-level information drives the model to converge with fewer training epochs. Consequently, the training time of CARE is comparable to or even shorter than its GNN counterparts.

The main contributions of this paper are summarized as follows:

- We put forward a novel graph representation refinement framework CARE, which considers class-aware graph-level relationships. CARE is a flexible plug-and-play framework that can incorporate arbitrary GNN models without significantly increasing the computational cost.
- We provide theoretic support through VC dimension analysis that CARE has better generalization upper bound in comparison with its GNN backbone.
- We perform extensive experiments using 10 GNN backbones on 9 benchmark datasets to justify the superiority of CARE on graph classification task in terms of both effectiveness and efficiency.

II. RELATED WORKS

A. Graph Neural Networks

Kipf and Welling [6] were the first to introduce the convolution operation to graphs. Later on, Hamilton et al. [7] proposed to use sampling and aggregation to learn node representations. The attention mechanism was introduced to graph convolution in [23] to yield node representations by unequally considering messages from different neighbors. The Graph Isomorphism Network (GIN) was proposed in [1], which has been shown to be as powerful as the Weisfeiler-Lehman (WL) test [24]. Recently, the transformer architecture [25] has been introduced to GNN [26], [27], which considers the relatedness between nodes in the node representation learning.

For GNN-based graph classification, graph pooling is commonly applied as the readout function to generate graph representations. Existing pooling methods can be categorised under node drop pooling [28]–[30] and node clustering pooling [2], [31]–[33]. Node drop pooling uses learnable scoring functions to drop nodes with lower scores while node clustering pooling casts the graph pooling problem into the node clustering problem [34]. In a recent development, Yang et al. [35] leverage

the mask mechanism to select the subgraph by considering the consistency over samples. Both categories of the pooling methods focus on node level manipulations and neglect the graph-level information.

B. Methods to Treat GNN Overfitting

Expressiveness of GNN could be improved by increasing the number of model parameters through e.g., expanding the hidden dimension of the GNN layer or adding more layers. However, this process could detriment the performance and induce overfitting [15].

A typical method to treat GNN overfitting is via data augmentation. Several works [16], [36] used node/edge dropping augmentations. [17] proposed a generator-classifier network under the adversarial learning setting to generate fake nodes. [37] performed adversarial perturbations to node features. Recently, the paradigm of contrastive learning has been introduced to GNN to perform graph contrastive learning [18], [38]. All these methods perform augmentation on individual graphs and again neglect the graph-level information.

Several resampling [19], [39] and reweighting [20], [40] methods have also been proposed to prevent GNN from overfitting. In general, these methods design algorithms to control the influence of each sample on the model, while the sample relations are not taken into account.

To the best of our knowledge, our work is the first to explore the use of class-aware graph-level relationships to alleviate the overfitting in GNNs.

III. OUR PROPOSED METHOD

In this section, we first give the problem formulation of graph classification, followed by the introduction of our proposed CARE framework. We also discuss two architectures for applying CARE to existing GNNs. Finally, we provide theoretic support for the generalization of CARE.

TABLE I
NOTATION TABLE

Notation	Description
G	An input graph
\mathbf{A}	Adjacency matrix of G
\mathbf{X}	Node feature matrix of G
\mathcal{V}_G	Node set of G
v	A node in G
n	Number of nodes in G
c	Dimensionality of node feature vector \mathbf{X}_v
\mathcal{D}	Input dataset
\mathcal{G}	Input graph set
\mathcal{Y}	Input label set
\mathcal{B}_i	Bag of (sub)graph representations of class i
y_G	Label of G
\mathbf{H}	Node representations
l	Number of layers in GNN
hg_G	Whole graph representation of G
\mathbf{H}_v	Node representation of v
m	Dimensionality of node representation \mathbf{H}_v
G_{sub}	Subgraph of G
\mathbf{A}_{sub}	Adjacency matrix of G_{sub}
\mathbf{H}_{sub}	Node representations of G_{sub}
i	i -th class in \mathcal{Y}
hc_i	Class representation of class i
hg'_G	Refined representation of G
\hat{y}	Predicted class label

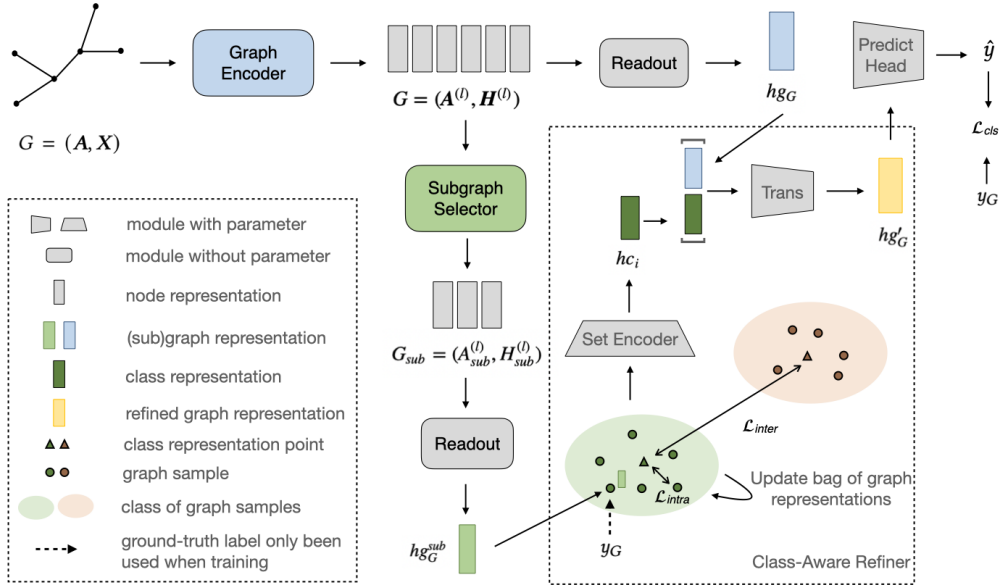


Fig. 1. Framework of CARE.

A. Problem Formulation

We represent a graph as $G = (A, X)$, where $A \in \{0, 1\}^{n \times n}$ is its adjacency matrix, and $X \in \mathbb{R}^{n \times c}$ denotes the feature matrix with each node characterized by a feature vector of c dimensions. The node set of G is denoted by \mathcal{V}_G and $|\mathcal{V}_G| = n$. We use X_v to denote the feature vector of a node $v \in \mathcal{V}_G$. Table I summarizes the notations used throughout the paper.

Given a data set of labeled graphs $\mathcal{D} = (\mathcal{G}, \mathcal{Y}) = \{(G, y_G)\}$, where $y_G \in \mathcal{Y}$ is the corresponding label of graph $G \in \mathcal{G}$, the problem of graph classification aims to learn a predictive function $f: \mathcal{G} \rightarrow \mathcal{Y}$ that maps graphs to their labels.

B. Class-Aware Representation Refinement Framework

We now describe our proposed Class-Aware Representation rEfinement framework (CARE), which aims to refine graph representations by considering the graph-level similarity. CARE contains four main components, including a graph encoder, a subgraph selector, a class-aware refiner and a class loss. The former two allow the flexible incorporation of existing GNN methods, while the latter two are newly proposed in our framework. Fig. 1 depicts the CARE framework.

The remainder of this section describes the four components in detail. We first introduce the graph encoder to get the initial node/graph representation, and then describe the subgraph selector to extract an appropriate substructure for the subsequent class representation learning. The class-aware refiner learns class representations from different graph classes, which are used to refine graph representations. A class loss is proposed to further improve class separability. The two new components in CARE only contain a small number of parameters and are easy to plugin arbitrary GNN backbone.

Graph Encoder A graph encoder extracts the node representations H and the graph-level representation hg_G for graph

G . CARE does not impose any constraint on the architecture of the graph encoder. Any message-passing GNN model could be applied here, which is formalized as:

$$\mathbf{H}_v^{(l+1)} = \text{UP}^{(l)} \left(\mathbf{H}_v^{(l)}, \text{AGG}^{(l)} \left(\left\{ \mathbf{H}_u^{(l)} \right\}_{u \in \mathcal{N}(v)} \right) \right), \quad (1)$$

where $\mathbf{H}^{(l+1)} \in \mathbb{R}^{n \times m}$ denotes the $(l+1)$ -th layer node representation with m dimensions, UP and AGG are arbitrary differentiable update and aggregate functions, $\mathcal{N}(v)$ represents the neighbor node set of node $v \in \mathcal{V}_G$, and $\mathbf{H}_v^{(0)}$ is initialized as the input feature vector X_v .

After a few message-passing layers, we can obtain a set of node representations. A READOUT function can be applied to produce the graph representation $hg_G \in \mathbb{R}^m$ as follows:

$$hg_G = \text{READOUT}(\{\mathbf{H}_v \mid v \in \mathcal{V}_G\}). \quad (2)$$

Subgraph Selector The class-aware refiner in CARE aims to maintain generic features for graph samples from different classes. However, the READOUT function in Eq. (2) treats all nodes equally without considering the class information. In fact, graphs in different classes are likely to have various substructures. To address this limitation, CARE introduces a subgraph selector $sub(\cdot)$ to filter nodes in the original graph, which is defined as follows:

$$A^{(l+1)}, H^{(l+1)} = sub(A^{(l)}, H^{(l)}). \quad (3)$$

Any graph pooling methods could be applied here to select subgraphs. Typical ones include node drop pooling methods [30] and node clustering pooling methods [34].

Class-Aware Refiner As existing GNN models ignore the relationships of graphs from different classes, a new component is designed in CARE to fill this gap. The class-aware

Algorithm 1 Training of Class-Aware Refiner

Input: Subgraph representation hg_G^{sub} of graph G (output by Subgraph Selector), graph representation hg_G , and ground-truth label y_G of G ;
Output: Refined graph representation hg'_G , intra-class loss \mathcal{L}_{intra} and inter-class loss \mathcal{L}_{inter} ;

- 1: Use hg_G^{sub} to update the bag of (sub)graph representations \mathcal{B}_i for $i = y_G$;
- 2: Calculate the class representation hc_i by Eq. (4);
- 3: Use hc_i and hg_G to obtain the refined graph representation hg'_G by Eq. (5);
- 4: Calculate the intra-class loss \mathcal{L}_{intra} and inter-class loss \mathcal{L}_{inter} by Eqs. (7) and (8);

refiner maintains a bag of encoded (sub)graph representations \mathcal{B}_i and aggregates these representations to obtain a class representation hc_i for each class $i \in \mathcal{Y}$. The aggregation function is a universal Set Encoder, e.g., DeepSets [41] or PointNet [42]. Herein, we apply DeepSets as in Eq. (4), in which $\rho(\cdot)$ is a multilayer perceptron (MLP) with a non-linear function ReLU, and $\phi(hg) = hg/|\mathcal{B}_i|$.

$$hc_i = \rho \left(\sum_{hg_G^{sub} \in \mathcal{B}_i} \phi(hg_G^{sub}) \right), \quad (4)$$

where hg_G^{sub} is the subgraph representation of a graph $G \in \mathcal{G}$, obtained by passing the output of the subgraph selector through the READOUT function in Eq. (2). The class representation hc_i is then used to refine graph representations for all graphs in the same class:

$$hg'_G = Trans([hg_G \mid hc_i]), \quad (5)$$

where $Trans(\cdot)$ is a transformation function and hg'_G is the refined graph representation. Herein, we set $Trans(\cdot) = \rho(\cdot)$.

In the validation and the test process, the ground truth label y_G is not available. The Class-Aware Refiner will predict a pseudo label \tilde{y}_G for graph G by classifying it to the most similar class and use the corresponding class representation for graph representation refinement. We use the cosine similarity as a metric to quantify the similarity between a graph representation and a class representation. The pseudo label is obtained as:

$$\tilde{y}_G = \arg \max_{i \in \mathcal{Y}} (cos_sim(hg_G^{sub}, hc_i)). \quad (6)$$

Note that class representations are kept unchanged in the validation/test process. The training algorithm of the class-aware refiner is summarized in Algorithm 1.

Class Loss For graph classification task, it would be beneficial to exploit the graph similarity within the same class and the graph discrepancy between different classes. This is essential for making different classes more separable. Using the classification loss only fails to learn such graph-level relations. Therefore, a class loss $\mathcal{L}_{class}(\cdot)$ is proposed in CARE to enforce the intra-class similarity and the inter-class

discrepancy. The former \mathcal{L}_{intra} is defined as the similarity between each graph representation and its class representation, while the latter \mathcal{L}_{inter} is defined as the similarity between different class representations. We again use the cosine similarity as a metric. The class loss \mathcal{L}_{class} is then defined as a function that maximizes \mathcal{L}_{intra} and minimizes \mathcal{L}_{inter} :

$$\mathcal{L}_{intra} = \text{AVG}_{i \in \mathcal{Y}} (\text{AVG}_{y_G=i} (cos_sim(hc_i, hg_G^{sub}))), \quad (7)$$

$$\mathcal{L}_{inter} = \text{AVG}_{i \in \mathcal{Y}} (\text{AVG}_{j > i, j \in \mathcal{Y}} (cos_sim(hc_i, hc_j))), \quad (8)$$

$$\mathcal{L}_{class} = \log \frac{\exp(\mathcal{L}_{inter})}{\exp(\mathcal{L}_{intra})}, \quad (9)$$

where $\text{AVG}(\cdot)$ is the average function.

The prediction of class label is still supervised by a classification loss $\mathcal{L}_{cls}(\cdot)$. Herein, we apply the commonly used cross-entropy loss [43], which is defined as:

$$\mathcal{L}_{cls} = \sum_{G \in \mathcal{G}} y_G \log (\hat{y}_G), \quad (10)$$

where \hat{y}_G is the predicted label for graph G .

The overall loss \mathcal{L} of the proposed CARE is defined as:

$$\mathcal{L} = \mathcal{L}_{cls} + \lambda * \mathcal{L}_{class}, \quad (11)$$

where λ is a trade-off hyperparameter for balancing the classification loss and the class loss.

C. Model Architecture Variants

As GNNs can be categorized as hierarchical ones and non-hierarchical ones, we design two corresponding architectures that apply CARE to plug-and-play in different GNN backbones.

Global Architecture Several GNN models (e.g., GCN [6], GAT [23] and GraphSAGE [7]) apply the readout function only at the end of graph convolution. The global architecture of CARE is designed to apply the Class-Aware Refiner only after the readout function. The outputs are then passed to the linear layer for graph classification.

Hierarchical Architecture Some other GNN models, such as GIN [1] and UGformer [26], have a readout function in each graph convolutional layer. The graph representations from each layer are taken into account when making the final prediction. The hierarchical architecture of CARE is designed to apply the class-aware refiner on each layer in order to cope with the hierarchical GNN backbones.

D. Generalization Analysis

In this section, we present the theoretical support that the proposed CARE has a better model generalization than its GNN backbone in the case of binary classification. We use the VC dimension to measure the capacity of a model. Based on the VC theory [44], reducing the VC dimension of a model has the effect of eliminating potential generalization errors.

Our analysis is grounded on the VC theory for neural nets [45]: the VC dimension of a neural network is upper bounded by a function with respect to the number of model parameters t and the number of operations p . In the following, we first derive the computational complexity of the GNN backbone and CARE measured by the number of multiplications, based on which we obtain an upper bound of the VC dimension for each model. We then present a theorem that states that CARE has a lower VC dimension upper bound than its GNN backbone when the number of parameters is identical. In subsequent discussions, we use GCN as an example backbone. The conclusion generally applies to other backbones by plugging in their corresponding computational complexity. We present the theoretical results here and defer the detailed proofs to Appendix.

Computational Complexity of Models. CARE and its backbone GCN are both composed of GCN layers, an embedding layer, and several fully-connected layers.

[*Complexity of GCN Backbone.*] We denote the GCN layer in the GCN model as $gcn(\cdot)$ and its input/output dimensions as $h_{gcn_{in}}/h_{gcn_{out}}$. The layer mapping is given by:

$$gcn(A, H) = \sigma_{gcn}(\hat{A}HW_{gcn}), \quad (12)$$

where σ_{gcn} is the activation function, $W_{gcn} \in \mathbb{R}^{h_{gcn_{in}} \times h_{gcn_{out}}}$ is the weight matrix, and \hat{A} is the normalized adjacency matrix. The computational complexity of the GCN network measured by the number of multiplications, denoted as $q_1(d)$, for d number of layers, is given by:

$$q_1(d) = \sum_{l=0}^d (n^2 h_{gcn_{in}}^l + nh_{gcn_{in}}^l h_{gcn_{out}}^l). \quad (13)$$

[*Complexity of CARE.*] The GCN-based CARE network with a hierarchical architecture is composed of the following:

- a GCN layer same as Eq. (12), whose computational complexity is $q_{gcn}^l = n^2 h_{gcn_{in}}^l + nh_{gcn_{in}}^l h_{gcn_{out}}^l$.
- a subgraph selector (SAGPool), which contains a score layer (GCN with 1 dimensional output) and a top-k pooling algorithm. The complexity is $q_{subgraph}^l = n^2 h_{gcn_{out}}^l + nh_{gcn_{out}}^l$.
- a class-aware refiner, which contains a set encoder Eq. (4) and a transformation layer Eq. (5). The mapping of the fully-connection layer $fc(\cdot)$ from input H is given by:

$$fc(H) = \sigma_{fc}(HW_{fc}), \quad (14)$$

where σ_{fc} is the activation function, $W_{fc} \in \mathbb{R}^{h_{fc_{in}} \times h_{fc_{out}}}$, and $h_{fc_{in}}/h_{fc_{out}}$ are the input/output dimensions. The complexities for the set encoder and the transformation layer are $q_{set}^l = nh_{set_{in}}^l h_{set_{out}}^l$ and $q_{trans}^l = nh_{trans_{in}}^l h_{trans_{out}}^l$, respectively.

Therefore, the computational complexity of the GCN-based CARE is given by:

$$q_2(d) = \sum_{l=0}^d (q_{gcn}^l + q_{subgraph}^l + q_{set}^l + q_{trans}^l). \quad (15)$$

VC Dimension Upper Bound. Inspired by the theoretical analysis in [46] that derives an upper bound of the VC dimension for a CNN model, we extend its result to a GCN model, as given by the following lemma.

Lemma 1 Let \mathcal{C}^d be the set of GCN models with d convolutional layers. Let $\mathcal{H}^d \triangleq \{h_c : I \rightarrow \{0, 1\} | c \in \mathcal{C}^d\}$ be the set of boolean functions implementable by all GCNs in \mathcal{C}^d . The VC dimension of GCNs, as well as CARE, satisfies:

$$VC_{dim}(\mathcal{H}^d) \leq \alpha(d \cdot q(d))^2, \quad (16)$$

for some constant α . Here, $q(d)$ is the computational complexity of the model under consideration.

VC Dimension Comparison We now compare the upper bounds of VC dimension on the GCN backbone and CARE, which is formalized by the following theorem.

Theorem 1. Assume that the number of parameters in a GCN backbone and CARE is identical. Let $upperVC(GCN)$ and $upperVC(CARE)$ be the upper bounds of VC dimension on the two models, respectively, which are given by Lemma 1. We have

$$upperVC(GCN) > upperVC(CARE). \quad (17)$$

Based on Theorem 1 and the VC theory, we conclude that our CARE has a better generalization potential than its GCN backbone.

IV. EXPERIMENTAL SETUP

In this section, we present the experimental setup, including datasets, GNN backbones and model implementation details.

A. Datasets

Nine commonly used benchmark datasets were tested in our experiments. Eight of them were selected from TUDataset [47] and include DD, PROTEINS, MUTAG, NCI1, NCI109, FRANKENSTEIN, Tox21 and ENZYMES. The last dataset OGBG-MOLHIV was selected from Open Graph Benchmark [48] and consists of 41K+ graphs. The statistics of the datasets are summarized in Table II.

B. GNN Backbones

We test the effectiveness of CARE on a wide range of GNN backbones, including GCN [6], GraphSAGE [7], GIN [1], GAT [23], UGformer [26], GXN [32], SAGPool [30], DiffPool [2], HGSPLPool [31] and MEWISPool [33]. We apply CARE on each of them and compare the performance with the original backbone model. Among the 10 models selected, GIN and UGformer are hierarchical ones. We thus apply the hierarchical architecture CARE on them. The global architecture CARE is applied to the rest models.

TABLE II
STATISTICS OF DATASETS.

Dataset	Graph#	Class#	Avg Node#	Avg Edge#
D&D	1178	2	284.32	715.66
PROTEINS	1113	2	39.06	72.82
MUTAG	188	2	17.93	19.79
NCI1	4110	2	29.87	32.30
NCI109	4127	2	29.68	32.13
FRANKENSTEIN	4337	2	16.90	17.88
Tox21	8169	2	18.09	18.50
ENZYMES	600	6	32.63	62.14
OGBG-MOLHIV	41127	2	25.50	27.50

C. Implementation Details

The default number of graph convolutional layers in both CARE and GNN backbones is 4. We use SAGPool with a pooling ratio of 0.5 as the default subgraph selector in CARE. Notice that we did not apply any subgraph selector on GNNs that are already equipped with their own pooling methods for substructure extraction. This includes SAGPool, DiffPool, HGPSLPool and MEWISPool. The trade-off hyperparameter λ in Eq. (11) is set to 1 by default. The whole network is trained in an end-to-end manner using the Adam optimizer [49]. We use the early stopping criterion, i.e., we stop the training once there is no further improvement on the validation loss during 25 epochs. The learning rate is initialized to 10^{-4} and the maximum number of epochs is set to 1000. We set the hidden size to 146 and batch size to 20 for all models. The only exception is DiffPool when tested on the D&D dataset. Since the D&D dataset has a large number of nodes (see Table II), the hidden size and batch size are set to 32 and 6 to achieve an acceptable number of parameters in DiffPool.

For each dataset, we split it into 8:1:1 for training, validation and test. For all experiments of CARE and GNN backbones, we evaluate each model with the same random seed for 10-fold cross-validation. The experiments were conducted in a Linux server with Intel(R) Core(TM) i9-10940X CPU (3.30GHz), GeForce GTX 3090 GPU, and 125GB RAM.

V. EXPERIMENTAL RESULTS

In this section, we first assess the performance of CARE in comparison with state-of-the-art GNN backbones. We then conduct ablation studies to analyze the effects of different components in CARE. A case study is presented to further investigate how CARE affects the separability of graphs from different classes. Finally, an evaluation of model efficiency is performed.

A. Performance Comparison with GNN Backbones

Effectiveness Analysis. We assess the graph classification performance on the first 8 datasets and the last dataset using two different metrics. The former is assessed by the classification accuracy and the latter by the ROC-AUC. This is because the OGBG-MOLHIV dataset has a severe class imbalance issue. The results on the first 8 datasets are reported in Table III. Each row in the table shows the performance of an original GNN backbone and the performance after applying CARE.

Each column reports the results on a dataset. In total there are 80 backbone/dataset pairs and the best result in each pair is highlighted in bold. As shown in Table III, CARE is a clear winner: it outperforms the GNN backbone in 74 out of 80 cases. CARE gains over 1% improvement in the absolute accuracy in 47 out of 74 winning cases, while it drops over 1% in accuracy in only 1 out of 6 losing cases. In particular, the improvement of CARE is up to 11.48%, which is achieved on the FRANKENSTEIN dataset with GraphSAGE as backbone. The same observation is made when testing on the OGBG-MOLHIV dataset using the scaffold splits. As shown in Table IV, CARE outperforms the GNN backbones in most cases with improvements up to 5.63%. To sum up, the results demonstrate that CARE is able to serve as a general framework to boost up the graph classification performance over state-of-the-art GNN models on various datasets.

Generalization Performance. We also observe that CARE is able to alleviate the overfitting in GNN backbones. An example is shown in Fig. 2, where we plot the accuracy curves on the PROTEINS dataset with GCN as the backbone. It shows that the test accuracy of GCN (in blue) exhibits a steep and continuous downward trend starting from epoch 120, while its corresponding training accuracy continues to climb up. This indicates an obvious overfit of GCN to the training data. After applying CARE on GCN (in red), the steep drop in the test accuracy vanishes, which demonstrates the ability of CARE in remitting overfitting.

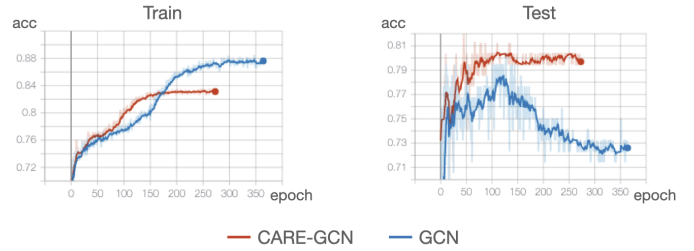


Fig. 2. Accuracy curves of CARE-GCN and GCN on PROTEINS dataset.

B. Ablation Studies

We perform two ablation studies to show how different designs of the Subgraph Selector and the loss function \mathcal{L} influence the performance of CARE.

Subgraph Selector We compare the performance of three CARE variants with different subgraph selectors on 5 datasets with 4 GNN backbones. The results are presented in Table V. The first CARE variant, denoted as "None", uses the whole graph for class representation learning without selecting any subgraph. The other two models apply SAGPool and HGSPLPool respectively as the subgraph selector. The pooling ratio for both SAGPool and HGSPLPool is set to 0.5. We can see that using the subgraph selector achieves the best result in 15 out of 20 cases. When comparing the performance of using SAGPool and HGSPLPool, the former beats the latter in 14 out of 20 cases. Therefore, we choose SAGPool as the default subgraph selector.

TABLE III

GRAPH CLASSIFICATION RESULTS (AVERAGE ACCURACY \pm STANDARD DEVIATION). WINNER IN EACH BACKBONE/DATASET PAIR IS HIGHLIGHTED IN BOLD.

Model		D&D	PROTEINS	MUTAG	NCI1	NCI109	FRANKENSTEIN	Tox21	ENZYMES
GraphSAGE	Original	72.18 \pm 2.93	74.87 \pm 3.38	75.48 \pm 6.11	63.94 \pm 2.53	65.46 \pm 1.12	52.95 \pm 4.01	88.36 \pm 0.15	52.50 \pm 5.69
	CARE	73.26 \pm 3.25	75.92 \pm 2.84	81.97 \pm 6.42	75.23 \pm 1.76	73.58 \pm 1.68	64.43 \pm 3.15	90.14 \pm 0.74	53.67 \pm 5.67
GCN	Original	71.02 \pm 3.17	73.89 \pm 2.85	77.52 \pm 10.81	78.80 \pm 2.01	75.06 \pm 2.50	55.58 \pm 0.11	88.14 \pm 0.29	62.17 \pm 6.33
	CARE	72.15 \pm 3.88	75.01 \pm 2.91	79.30 \pm 11.81	79.66 \pm 1.71	75.75 \pm 1.63	59.15 \pm 2.25	90.31 \pm 0.56	65.00 \pm 5.63
GIN	Original	73.10 \pm 2.44	72.41 \pm 4.45	89.36 \pm 4.71	81.96 \pm 2.03	81.01 \pm 1.84	67.23 \pm 1.93	92.10 \pm 0.59	62.79 \pm 7.64
	CARE	74.70 \pm 3.37	72.32 \pm 4.25	90.44 \pm 4.58	82.34 \pm 2.11	82.15 \pm 1.79	67.33 \pm 2.74	92.43 \pm 0.78	68.17 \pm 7.05
GAT	Original	74.25 \pm 3.76	74.34 \pm 2.09	77.56 \pm 10.49	78.07 \pm 1.94	74.34 \pm 2.18	62.85 \pm 1.90	90.35 \pm 0.71	67.67 \pm 3.74
	CARE	75.38 \pm 2.93	76.72 \pm 1.74	77.69 \pm 8.99	78.52 \pm 2.12	76.39 \pm 2.76	62.57 \pm 2.37	90.76 \pm 0.73	69.17 \pm 5.02
GXN	Original	67.62 \pm 5.85	70.32 \pm 3.03	83.22 \pm 7.97	73.34 \pm 2.54	72.18 \pm 2.24	60.86 \pm 2.17	89.93 \pm 0.73	63.13 \pm 4.68
	CARE	69.24 \pm 6.97	72.70 \pm 2.73	84.24 \pm 8.53	74.75 \pm 2.90	73.78 \pm 1.66	62.64 \pm 2.27	90.16 \pm 0.85	64.44 \pm 6.96
UGformer	Original	75.51 \pm 3.92	70.17 \pm 5.42	75.66 \pm 8.67	68.84 \pm 1.54	66.37 \pm 2.74	56.13 \pm 2.51	88.06 \pm 0.50	64.57 \pm 4.53
	CARE	76.23 \pm 4.45	71.84 \pm 3.87	77.66 \pm 5.93	67.03 \pm 1.69	66.92 \pm 1.58	57.10 \pm 2.27	88.21 \pm 0.24	65.24 \pm 5.91
SAGPool	Original	71.46 \pm 3.60	74.12 \pm 3.46	78.12 \pm 8.35	78.34 \pm 1.96	76.15 \pm 2.25	59.07 \pm 2.23	90.78 \pm 0.63	62.00 \pm 4.76
	CARE	73.28 \pm 2.25	74.75 \pm 3.14	79.81 \pm 7.52	78.91 \pm 2.21	76.44 \pm 1.74	59.67 \pm 2.04	90.64 \pm 0.38	63.17 \pm 4.37
DiffPool	Original	70.45 \pm 2.54	72.18 \pm 2.80	85.26 \pm 4.79	79.78 \pm 2.11	76.98 \pm 1.88	65.01 \pm 3.17	91.02 \pm 0.37	48.33 \pm 6.67
	CARE	72.90 \pm 4.58	72.57 \pm 2.97	86.33 \pm 8.14	80.47 \pm 1.67	78.49 \pm 1.72	64.36 \pm 3.43	91.58 \pm 0.65	51.17 \pm 6.75
HGPSLPool	Original	71.25 \pm 3.25	73.06 \pm 3.20	80.82 \pm 6.63	79.26 \pm 1.44	75.83 \pm 1.98	60.82 \pm 2.85	90.12 \pm 0.47	63.33 \pm 5.06
	CARE	71.61 \pm 3.36	75.47 \pm 3.98	82.31 \pm 6.91	79.77 \pm 1.97	76.87 \pm 1.94	63.36 \pm 1.73	90.44 \pm 0.69	66.00 \pm 4.48
MEWISPool	Original	76.03 \pm 2.59	68.10 \pm 3.97	84.73 \pm 4.73	74.21 \pm 3.26	75.30 \pm 1.45	64.63 \pm 2.83	88.13 \pm 0.05	53.66 \pm 6.07
	CARE	75.18 \pm 3.90	69.64 \pm 3.69	85.39 \pm 5.85	76.48 \pm 2.74	75.34 \pm 2.86	65.39 \pm 1.67	88.65 \pm 0.07	55.67 \pm 6.33

TABLE IV

GRAPH CLASSIFICATION RESULTS (AVERAGE ROC-AUC \pm STANDARD DEVIATION) ON OGBG-MOLHIV DATASET. WINNER IN EACH BACKBONE/DATASET PAIR IS HIGHLIGHTED IN BOLD.

GraphSAGE	GCN	GIN	GAT	GXN	UGformer	SAGPool	DiffPool	HGPSLPool	MEWISPool
Original	70.37 \pm 0.42	73.49 \pm 1.99	65.11 \pm 2.56	75.83 \pm 1.78	69.15 \pm 0.01	77.23 \pm 3.54	73.80 \pm 1.86	71.63 \pm 2.25	76.08 \pm 2.86
CARE	74.33 \pm 2.12	74.29 \pm 1.07	65.42 \pm 3.70	76.89 \pm 2.18	69.17 \pm 0.02	78.04 \pm 3.19	74.42 \pm 1.53	70.21 \pm 2.79	77.23 \pm 2.16

TABLE V

ABLATION STUDY ON DIFFERENT SUBGRAPH SELECTORS. WINNER IN EACH BACKBONE/DATASET PAIR IS HIGHLIGHTED IN BOLD.

Backbone	Subgraph Selector	D&D	PROTEINS	MUTAG	NCI1	NCI109
GraphSAGE	None	67.24 \pm 4.64	75.01 \pm 4.15	82.95 \pm 5.86	77.66 \pm 1.98	73.67 \pm 1.28
	SAGPool	73.26 \pm 3.25	75.92 \pm 2.84	81.97 \pm 6.42	75.23 \pm 1.76	73.58 \pm 1.68
	HGPSLPool	71.82 \pm 3.99	75.28 \pm 3.76	77.57 \pm 7.33	75.84 \pm 1.50	74.36 \pm 2.17
GCN	None	71.05 \pm 3.89	73.39 \pm 3.45	78.74 \pm 9.67	79.15 \pm 1.66	76.30 \pm 2.31
	SAGPool	72.15 \pm 3.88	75.01 \pm 2.91	79.30 \pm 11.81	79.66 \pm 1.71	75.75 \pm 1.63
	HGPSLPool	68.75 \pm 3.45	73.39 \pm 3.45	77.66 \pm 5.13	79.25 \pm 1.90	75.35 \pm 2.57
GIN	None	75.64 \pm 3.38	71.96 \pm 5.49	88.80 \pm 5.05	82.85 \pm 1.27	82.11 \pm 1.60
	SAGPool	74.70 \pm 3.37	72.32 \pm 4.25	90.44 \pm 4.58	82.34 \pm 2.11	82.15 \pm 1.79
	HGPSLPool	75.06 \pm 3.49	72.86 \pm 4.66	90.47 \pm 6.10	81.63 \pm 1.80	81.05 \pm 1.10
GAT	None	74.28 \pm 2.43	75.74 \pm 2.88	78.22 \pm 6.77	75.30 \pm 3.01	74.90 \pm 2.24
	SAGPool	75.38 \pm 2.93	76.72 \pm 1.74	77.69 \pm 8.99	78.52 \pm 2.12	76.39 \pm 2.76
	HGPSLPool	74.79 \pm 2.73	75.46 \pm 3.56	79.33 \pm 9.73	75.74 \pm 2.32	74.15 \pm 3.53

Class Loss We investigate different designs of the loss function to study the impact of the class loss proposed in this paper. We consider four designs of the overall loss function \mathcal{L} : a) *cls*: uses the classification loss in Eq. (10) only; b) *intra*: uses a combination of the classification loss and the intra-class loss as given by Eq. (18); c) *inter*: uses a combination of the classification loss and the inter-class loss as given by Eq. (19); and d) *class*, the proposed overall loss function in Eq. (11). The results in Table VI show that the proposed loss function performs the best among all designs. This demonstrates the effectiveness of the proposed class loss that takes into account the intra-class similarity and inter-class discrepancy.

$$\mathcal{L} = \mathcal{L}_{cls} - \lambda * \log \exp(\mathcal{L}_{intra}) \quad (18)$$

$$\mathcal{L} = \mathcal{L}_{cls} + \lambda * \log \exp(\mathcal{L}_{inter}) \quad (19)$$

TABLE VI

ABLATION STUDY ON DESIGN OF LOSS FUNCTION. WINNER IN EACH BACKBONE/DATASET PAIR IS HIGHLIGHTED IN BOLD.

Backbone	Loss	D&D	PROTEINS	MUTAG
GraphSAGE	<i>cls</i>	72.24 \pm 2.72	75.82 \pm 3.34	75.50 \pm 6.05
	<i>intra</i>	70.12 \pm 3.27	75.83 \pm 2.83	77.02 \pm 10.45
	<i>inter</i>	70.30 \pm 3.61	75.02 \pm 3.55	81.87 \pm 7.67
	<i>class</i>	73.26 \pm 3.25	75.92 \pm 2.84	81.97 \pm 6.42
GCN	<i>cls</i>	71.39 \pm 2.81	74.21 \pm 2.74	77.11 \pm 9.48
	<i>intra</i>	71.89 \pm 5.35	74.65 \pm 4.10	78.22 \pm 7.17
	<i>inter</i>	71.31 \pm 2.06	74.20 \pm 3.88	78.18 \pm 10.41
	<i>class</i>	72.15 \pm 3.88	75.01 \pm 2.91	79.30 \pm 11.81

C. Case Study for Class Separability

We design a case study to further investigate the effect of CARE, in particular its class-aware components, in refining graph representations for the classification task. The idea is to study how CARE affects the separability of graph classes in

TABLE VII

TIME EFFICIENCY OF CARE AND BACKBONES . TOTAL TIME WAS RECORDED FOR A SINGLE RUN (INCLUDING TRAINING, VALIDATION, AND TEST) WITH BATCH SIZE 20 AND 10-FOLD CV. BEST TIME IN EACH BACKBONE/DATASET PAIR IS HIGHLIGHTED IN BOLD.

Model	D&D		PROTEINS		MUTAG		
	Epoch # \pm s.d.	Total Time (h)	Epoch # \pm s.d.	Total Time (h)	Epoch # \pm s.d.	Total Time (h)	
GraphSAGE	Original	500.6 \pm 123.2	1.2050	320.5 \pm 53.2	1.2093	384.1 \pm 101.3	0.1798
	CARE	293.5 \pm 12.0	1.1422	282.0 \pm 51.5	0.9113	302.2 \pm 34.1	0.1593
GCN	Original	267.4 \pm 3.4	0.6920	365.0 \pm 27.9	0.6699	352.4 \pm 69.9	0.1318
	CARE	264.1 \pm 5.2	0.8476	306.5 \pm 17.2	0.6645	332.4 \pm 57.3	0.1425

the training process. Is it able to direct the graph representation learning to move towards better class separability? In order to answer this question, we use four class separability metrics as follows. For all metrics, the larger their values, the better the class separability is.

Silhouette Coefficient [50] It measures how similar a sample is to its own class (cohesion) compared to those from other classes (separation). Its value ranges from -1 to 1.

Separability Index [51] It computes the fraction of samples that have a nearest neighbour with the same class label. Its value ranges from 0 to 1.

Hypothesis Margin [52] It measures the distance between a sample’s nearest neighbor from the same class (near-hit) and the nearest neighbor from the opposing class (near-miss) and averages over all samples.

Centroid Distance It sums up the distances between the centroids for all pairs of classes, where the centroid of a class is the mean of all samples in the class.

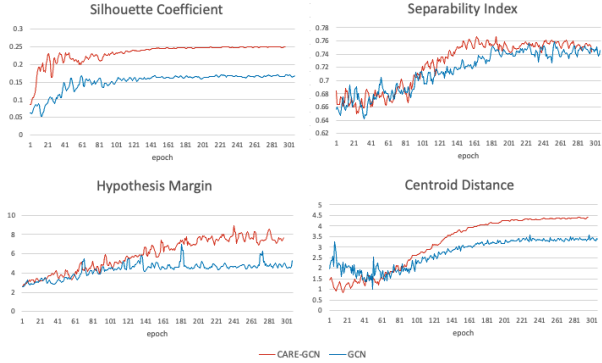


Fig. 3. Class Separability on PROTEINS with GCN Backbone (Training Set).

Fig. 3 reports the results on the PROTEINS dataset with GCN as the backbone. We compute the four metrics on the graph representations produced by CARE and GCN on the training data. CARE uses the refined graph representations, while GCN uses the original ones. It can be seen that the training curves of CARE exhibit an upward trend under all the four separability metrics. At the time when models converge, CARE outperforms GCN in all metrics. In particular, CARE achieves 49.26% improvement on Silhouette Coefficient, 1.96% on Separability Index, 45.21% on Hypothesis Margin, and 30.51% on centroid distance. A visualization of the graph representations in each model is shown in Fig. 5. Graph representations are passed into T-SNE [53] for

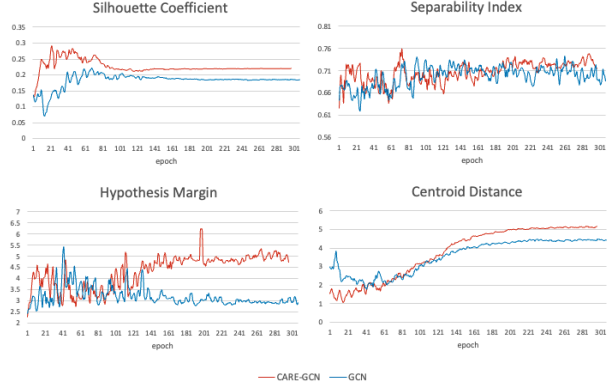


Fig. 4. Class Separability on PROTEINS with GCN Backbone (Test Set). The results were obtained by passing the test data once at the end of each training epoch. Note that this process doesn’t affect the training in any way as the model parameters/loss are not updated when passing the test data.

dimensionality reduction and colored by their class labels. This demonstrates that CARE is indeed able to steer the graph representation learning towards better class separability, which is also reflected by its superior classification performance over GNN backbones. Similar conclusions can be drawn from the results on the test data (Fig. 4), which indicates that the class separability of CARE generalizes well to the test data.

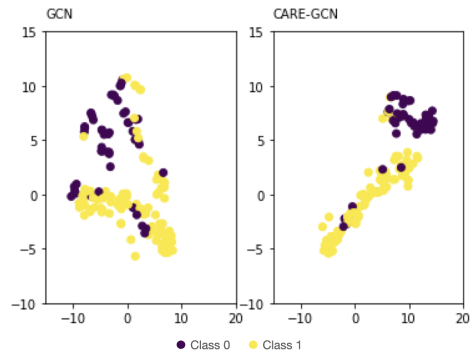


Fig. 5. Visualization of Graph Representations Produced by GCN and CARE-GCN on PROTEINS dataset.

D. Time Efficiency

CARE, when applied to a GNN backbone, introduces an additional refiner and the class loss. A natural question arises: will CARE significantly sacrifice the efficiency of its GNN backbone for better classification performance? This

subsection aims to answer this question. Table VII reports the number of epochs and the total time needed (including training, validation and test) for CARE and the backbones GraphSAGE and GCN. It can be seen that CARE takes less number of epochs to converge than its GNN counterpart in all cases. Consequently, the running time of CARE is shorter than (4 out of 6 cases) or comparable to its backbones. The results demonstrate that CARE is able to work on top of existing GNN models with superior effectiveness and improved/comparable efficiency, making it a practical choice in real applications.

VI. CONCLUSIONS

In this paper, we proposed CARE, a novel graph representation refinement framework for GNN-based graph classification. It fills the gap that existing GNNs fail to consider graph-level relationships in model design, and meanwhile improves the model generalization as proven theoretically and evidenced empirically. Its plug-in-play nature makes it a powerful framework to build upon arbitrary GNN models and boost up their classification performance without sacrificing efficiency. In the future, it is an interesting direction to explore the incorporation of graph-level information in the context of self-supervised graph learning.

REFERENCES

- [1] K. Xu, W. Hu, J. Leskovec, and S. Jegelka, “How powerful are graph neural networks?” in *International Conference on Learning Representations*, 2018.
- [2] R. Ying, J. You, C. Morris, X. Ren, W. L. Hamilton, and J. Leskovec, “Hierarchical graph representation learning with differentiable pooling,” *arXiv preprint arXiv:1806.08804*, 2018.
- [3] M. Zhang and Y. Chen, “Link prediction based on graph neural networks,” *Advances in neural information processing systems*, vol. 31, 2018.
- [4] T. N. Kipf and M. Welling, “Variational graph auto-encoders,” *arXiv preprint arXiv:1611.07308*, 2016.
- [5] X. Zhang, H. Liu, Q. Li, and X.-M. Wu, “Attributed graph clustering via adaptive graph convolution,” *arXiv preprint arXiv:1906.01210*, 2019.
- [6] T. N. Kipf and M. Welling, “Semi-supervised classification with graph convolutional networks,” *arXiv preprint arXiv:1609.02907*, 2016.
- [7] W. L. Hamilton, R. Ying, and J. Leskovec, “Inductive representation learning on large graphs,” in *Proceedings of the 31st International Conference on Neural Information Processing Systems*, 2017, pp. 1025–1035.
- [8] W. Fan, Y. Ma, Q. Li, Y. He, E. Zhao, J. Tang, and D. Yin, “Graph neural networks for social recommendation,” in *The world wide web conference*, 2019, pp. 417–426.
- [9] H. Dai, B. Dai, and L. Song, “Discriminative embeddings of latent variable models for structured data,” in *International conference on machine learning*. PMLR, 2016, pp. 2702–2711.
- [10] J. Gilmer, S. S. Schoenholz, P. F. Riley, O. Vinyals, and G. E. Dahl, “Neural message passing for quantum chemistry,” in *International conference on machine learning*. PMLR, 2017, pp. 1263–1272.
- [11] S. Wu, F. Sun, W. Zhang, and B. Cui, “Graph neural networks in recommender systems: a survey,” *arXiv preprint arXiv:2011.02260*, 2020.
- [12] W. Xia, Y. Li, J. Tian, and S. Li, “Forecasting interaction order on temporal graphs,” in *Proceedings of the 27th ACM SIGKDD Conference on Knowledge Discovery & Data Mining*, 2021, pp. 1884–1893.
- [13] B.-H. Kim and J. C. Ye, “Understanding graph isomorphism network for rs-fmri functional connectivity analysis,” *Frontiers in neuroscience*, p. 630, 2020.
- [14] Z. Wu, S. Pan, F. Chen, G. Long, C. Zhang, and S. Y. Philip, “A comprehensive survey on graph neural networks,” *IEEE transactions on neural networks and learning systems*, vol. 32, no. 1, pp. 4–24, 2020.
- [15] X. Song, R. Ma, J. Li, M. Zhang, and D. P. Wipf, “Network in graph neural network,” *arXiv preprint arXiv:2111.11638*, 2021.
- [16] P. A. Papp, K. Martinkus, L. Faber, and R. Wattenhofer, “Dropgnn: random dropouts increase the expressiveness of graph neural networks,” *Advances in Neural Information Processing Systems*, vol. 34, 2021.
- [17] M. Ding, J. Tang, and J. Zhang, “Semi-supervised learning on graphs with generative adversarial nets,” in *Proceedings of the 27th ACM International Conference on Information and Knowledge Management*, 2018, pp. 913–922.
- [18] Y. You, T. Chen, Y. Sui, T. Chen, Z. Wang, and Y. Shen, “Graph contrastive learning with augmentations,” *Advances in Neural Information Processing Systems*, vol. 33, pp. 5812–5823, 2020.
- [19] J. Byrd and Z. Lipton, “What is the effect of importance weighting in deep learning?” in *International Conference on Machine Learning*. PMLR, 2019, pp. 872–881.
- [20] T.-Y. Lin, P. Goyal, R. Girshick, K. He, and P. Dollár, “Focal loss for dense object detection,” in *Proceedings of the IEEE international conference on computer vision*, 2017, pp. 2980–2988.
- [21] Y. Wen, K. Zhang, Z. Li, and Y. Qiao, “A discriminative feature learning approach for deep face recognition,” in *European conference on computer vision*. Springer, 2016, pp. 499–515.
- [22] V. N. Vapnik and A. Y. Chervonenkis, “On the uniform convergence of relative frequencies of events to their probabilities,” in *Measures of complexity*. Springer, 2015, pp. 11–30.
- [23] P. Veličković, G. Cucurull, A. Casanova, A. Romero, P. Lio, and Y. Bengio, “Graph attention networks,” *arXiv preprint arXiv:1710.10903*, 2017.
- [24] B. Weisfeiler and A. Leman, “The reduction of a graph to canonical form and the algebra which appears therein,” *NTI, Series*, vol. 2, no. 9, pp. 12–16, 1968.
- [25] A. Vaswani, N. Shazeer, N. Parmar, J. Uszkoreit, L. Jones, A. N. Gomez, Ł. Kaiser, and I. Polosukhin, “Attention is all you need,” in *Advances in neural information processing systems*, 2017, pp. 5998–6008.
- [26] D. Q. Nguyen, T. D. Nguyen, and D. Phung, “Universal graph transformer self-attention networks,” *arXiv preprint arXiv:1909.11855*, 2019.
- [27] Y. Rong, Y. Bian, T. Xu, W. Xie, Y. Wei, W. Huang, and J. Huang, “Grover: Self-supervised message passing transformer on large-scale molecular data,” *Advances in Neural Information Processing Systems*, 2020.
- [28] D. K. Duvenaud, D. Maclaurin, J. Iparragirre, R. Bombarell, T. Hirzel, A. Aspuru-Guzik, and R. P. Adams, “Convolutional networks on graphs for learning molecular fingerprints,” *Advances in neural information processing systems*, vol. 28, 2015.
- [29] M. Zhang, Z. Cui, M. Neumann, and Y. Chen, “An end-to-end deep learning architecture for graph classification,” in *Thirty-Second AAAI Conference on Artificial Intelligence*, 2018.
- [30] J. Lee, I. Lee, and J. Kang, “Self-attention graph pooling,” in *International Conference on Machine Learning*. PMLR, 2019, pp. 3734–3743.
- [31] Z. Zhang, J. Bu, M. Ester, J. Zhang, C. Yao, Z. Yu, and C. Wang, “Hierarchical graph pooling with structure learning,” *arXiv preprint arXiv:1911.05954*, 2019.
- [32] M. Li, S. Chen, Y. Zhang, and I. W. Tsang, “Graph cross networks with vertex infomax pooling,” *arXiv preprint arXiv:2010.01804*, 2020.
- [33] A. Nouranizadeh, M. Matinkia, M. Rahmati, and R. Safabakhsh, “Maximum entropy weighted independent set pooling for graph neural networks,” *arXiv preprint arXiv:2107.01410*, 2021.
- [34] J. Baek, M. Kang, and S. J. Hwang, “Accurate learning of graph representations with graph multiset pooling,” *arXiv preprint arXiv:2102.11533*, 2021.
- [35] M. Yang, Y. Shen, H. Qi, and B. Yin, “Soft-mask: Adaptive substructure extractions for graph neural networks,” in *Proceedings of the Web Conference 2021*, 2021, pp. 2058–2068.
- [36] Y. Rong, W. Huang, T. Xu, and J. Huang, “Dropedge: Towards deep graph convolutional networks on node classification,” *arXiv preprint arXiv:1907.10903*, 2019.
- [37] F. Feng, X. He, J. Tang, and T.-S. Chua, “Graph adversarial training: Dynamically regularizing based on graph structure,” *IEEE Transactions on Knowledge and Data Engineering*, vol. 33, no. 6, pp. 2493–2504, 2019.
- [38] S. Thakoor, C. Tallec, M. G. Azar, R. Munos, P. Veličković, and M. Valko, “Bootstrapped representation learning on graphs,” *arXiv preprint arXiv:2102.06514*, 2021.
- [39] Q. Zhou, B. Sun, Y. Song, and S. Li, “K-means clustering based undersampling for lower back pain data,” in *Proceedings of the 2020 3rd International Conference on Big Data Technologies*, 2020, pp. 53–57.

- [40] S. Shi, K. Qiao, S. Yang, L. Wang, J. Chen, and B. Yan, “Boosting-gnn: Boosting algorithm for graph networks on imbalanced node classification,” *Frontiers in neurorobotics*, p. 154, 2021.
- [41] M. Zaheer, S. Kottur, S. Ravanbakhsh, B. Poczos, R. R. Salakhutdinov, and A. J. Smola, “Deep sets,” *Advances in neural information processing systems*, vol. 30, 2017.
- [42] C. R. Qi, H. Su, K. Mo, and L. J. Guibas, “Pointnet: Deep learning on point sets for 3d classification and segmentation,” *computer vision and pattern recognition*, 2016.
- [43] D. R. Cox, “The regression analysis of binary sequences,” *Journal of the Royal Statistical Society: Series B (Methodological)*, vol. 20, no. 2, pp. 215–232, 1958.
- [44] V. Vapnik, “The nature of statistical learning theory (information science and statistics) springer-verlag,” *New York*, 2000.
- [45] P. L. Bartlett and W. Maass, “Vapnik-chervonenkis dimension of neural nets,” *The handbook of brain theory and neural networks*, pp. 1188–1192, 2003.
- [46] M. Kabkab, E. Hand, and R. Chellappa, “On the size of convolutional neural networks and generalization performance,” in *2016 23rd International Conference on Pattern Recognition (ICPR)*. IEEE, 2016, pp. 3572–3577.
- [47] K. Kersting, N. M. Kriege, C. Morris, P. Mutzel, and M. Neumann, “Benchmark data sets for graph kernels,” 2016. [Online]. Available: <http://graphkernels.cs.tu-dortmund.de>
- [48] W. Hu, M. Fey, M. Zitnik, Y. Dong, H. Ren, B. Liu, M. Catasta, and J. Leskovec, “Open graph benchmark: Datasets for machine learning on graphs,” *Advances in neural information processing systems*, vol. 33, pp. 22 118–22 133, 2020.
- [49] D. P. Kingma and J. Ba, “Adam: A method for stochastic optimization,” *arXiv preprint arXiv:1412.6980*, 2014.
- [50] P. J. Rousseeuw, “Silhouettes: a graphical aid to the interpretation and validation of cluster analysis,” *Journal of computational and applied mathematics*, vol. 20, pp. 53–65, 1987.
- [51] C. Thornton, “Separability is a learner’s best friend,” in *4th Neural Computation and Psychology Workshop, London, 9–11 April 1997*. Springer, 1998, pp. 40–46.
- [52] R. Gilad-Bachrach, A. Navot, and N. Tishby, “Margin based feature selection-theory and algorithms,” in *Proceedings of the twenty-first international conference on Machine learning*, 2004, p. 43.
- [53] L. Van der Maaten and G. Hinton, “Visualizing data using t-sne.” *Journal of machine learning research*, vol. 9, no. 11, 2008.

APPENDIX

A. Proof Sketch of Lemma 1

Our proof follows the same flow as Lemma 1 in [46].

A parametrized class of functions with parameters in \mathbb{R}^t that is computable in no more than p operations has a VC dimension which is $O(t^2p^2)$ [45]. t in GCN and CARE can be formulated as:

$$t_{GCN} = \sum_{l=0}^d h_{gcn_{in}}^l h_{gcn_{out}}^l; \quad (20)$$

$$t_{CARE} = \sum_{l=0}^d (h_{gcn_{in}}^l h_{gcn_{out}}^l + h_{gcn_{out}}^l + h_{set_{in}}^l h_{set_{out}}^l + h_{trans_{in}}^l h_{trans_{out}}^l). \quad (21)$$

By plugging in the number of multiplications $q_1(d)$ and $q_2(d)$ given by Eqs. (13) and (15), together with the above equations on the number of parameters t , into $O(t^2p^2)$, we complete the proof of Lemma 1 for both GCN and CARE.

B. Proof of Theorem 1

We compare the VC dimension upper bounds of a GCN layer and a GCN-based CARE layer under the identical number of parameters. The number of parameters in a GCN layer t_1 and that in a GCN-based CARE layer t_2 are formulated as:

$$t_1 = h_{gcn_{in}} h_{gcn_{out}}, \quad (22)$$

$$t_2 = h_{gcn_{in}} h_{gcn_{out}} + h_{gcn_{out}} + h_{set_{in}} h_{set_{out}} + h_{trans_{in}} h_{trans_{out}}. \quad (23)$$

In our setting, we choose a basic hidden dimension h_1 and h_2 for GCN and CARE respectively. We set each layer to be an integer multiple of the basic hidden dimension. Thus, $t_1 = h_1^2$ and $t_2 = h_2^2 + h_2 + h_2^2 + 2h_2^2 = 4h_2^2 + h_2$, respectively.

Note that $h_{trans_{in}} = h_{set_{out}} + h_{gcn_{out}}$ as we concatenate the class representation with the subgraph representation.

Similarly, the computational complexities q_1 and q_2 can be rewritten as:

$$q_1(d) = \sum_{l=0}^d (nh_1^2 + n^2h_1), \quad (24)$$

$$q_2(d) = \sum_{l=0}^d (4nh_2^2 + (2n^2 + n)h_2). \quad (25)$$

When $d = 1$, the complexity can be written as:

$$q_1(1) = nh_1^2 + n^2h_1, \quad (26)$$

$$q_2(1) = 4nh_2^2 + (2n^2 + n)h_2. \quad (27)$$

Under the identical number of parameters, we let $t_1 = t_2$, and have $h_1 = \sqrt{4h_2^2 + h_2}$. Thus,

$$q_1(1) = 4nh_2^2 + nh_2 + n^2\sqrt{4h_2^2 + h_2}. \quad (28)$$

The difference between $q_1(1)$ and $q_2(1)$ satisfies:

$$q_1(1) - q_2(1) = n^2(\sqrt{4h_2^2 + h_2} - 2h_2). \quad (29)$$

Because $\sqrt{4h_2^2 + h_2} - 2h_2 > 0$, we have:

$$q_1(1) > q_2(1). \quad (30)$$

According to our setting, the input and output feature map sizes of all layers is identical, which means that the ‘ n ’ in each layer’s complexity equation are identical. Thus, we extend Eq. (30) to the full model and have:

$$q_1(d) > q_2(d). \quad (31)$$

With Eq. (31) and Lemma 1, we complete the proof of Theorem 1.